Supplementary Information: Morphology and band structure of orthorhombic PbS nanoplatelets: an indirect band gap material

David F. Macias-Pinilla,[†,‡] Carlos Echeverría-Arrondo,[‡] Andrés. F. Gualdrón-Reyes,[‡] Said Agouram,[¶,§] Vicente Muñoz-Sanjosé,[¶,§] Josep Planelles,[†] Iván Mora-Seró,[‡,§] and Juan I. Climente[*,†]

†*Departament de Química Física i Analítica, Universitat Jaume I, Av. Sos Baynat, s/n, 12071 Castelló, Spain*

‡*Institute of Advanced Materials (INAM), Universitat Jaume I, Av. Sos Baynat, s/n, 12071 Castelló, Spain*

¶*Department of Applied Physics and Electromagnetism, University of Valencia, 46100 Valencia, Spain*

§*Materials for Renewable Energy (MAER), Unitat Mixa d'Investigació UV-UJI*

E-mail: climente@uji.es

PbS Rock-Salt Effective Masses via k · p Model

In order to understand the photophysics of the PbS rock-salt NPLs we take advantage of the Dimmock Hamiltonian, which is the expansion of the $k \cdot p$ Hamiltonian, including valence-conduction interaction, anisotropies, self polarization potential and SOC.[1] A full view of the model used in PbS rock-salt structures can be found in the supplementary information of Ref. 2. Rock-salt PbS has direct bandgap at L point (center of the hexagonal face of

the first Brillouin zone). With z in the cubic lattice direction [111], the valence band (VB) edge Bloch function has L_6^+ symmetry (s-like) and the conduction band (CB) edge Bloch function has L_6^- symmetry (p_z-like). With theses considerations we can write the Dimmock Hamiltonian as a 4×4 matrix (conduction and valence - spin up, spin down)[1]

$$H = \begin{bmatrix} \frac{E_g}{2} + \frac{\hbar^2 k_t^2}{2m_t^-} + \frac{\hbar^2 k_z^2}{2m_l^-} & 0 & \frac{\hbar}{m} P_l k_z & \frac{\hbar}{m} P_t (k_x - i k_y) \\ 0 & \frac{E_g}{2} + \frac{\hbar^2 k_t^2}{2m_t^-} + \frac{\hbar^2 k_z^2}{2m_l^-} & \frac{\hbar}{m} P_t (k_x + i k_y) & -\frac{\hbar}{m} P_l k_z \\ \frac{\hbar}{m} P_l k_z & \frac{\hbar}{m} P_t (k_x - i k_y) & -\frac{E_g}{2} - \frac{\hbar^2 k_t^2}{2m_t^+} - \frac{\hbar^2 k_z^2}{2m_l^+} & 0 \\ \frac{\hbar}{m} P_t (k_x + i k_y) & -\frac{\hbar}{m} P_l k_z & 0 & -\frac{E_g}{2} - \frac{\hbar^2 k_t^2}{2m_t^+} - \frac{\hbar^2 k_z^2}{2m_l^+} \end{bmatrix}, \quad (1)$$

where E_g is the band gap, m is the free electron mass, P_t and P_l are the transverse and longitudinal Kane parameters, $m_t^\pm$ and $m_l^\pm$ are the transverse and longitudinal band-edge effective masses for electron ($-$) and hole ($+$), and k_i are momentum operators.

Hamiltonian in eq. (1) can be written in compact form as in Ref. 3

$$H = \begin{bmatrix} (\frac{E_g}{2} + \frac{\hbar^2 k_t^2}{2m_t^-} + \frac{\hbar^2 k_z^2}{2m_l^-}) \mathbb{1} & \frac{\hbar}{m} P_l k_z \sigma_z + \frac{\hbar}{m} P_t k_t \sigma_t \\ \frac{\hbar}{m} P_l k_z \sigma_z + \frac{\hbar}{m} P_t k_t \sigma_t & (-\frac{E_g}{2} - \frac{\hbar^2 k_t^2}{2m_t^+} - \frac{\hbar^2 k_z^2}{2m_l^+}) \mathbb{1} \end{bmatrix},$$

where σ_x, σ_y and σ_z are the Pauli matrices, $k_t = (k_x, k_y)$, $\sigma_t = (\sigma_x, \sigma_y)$, and $\mathbb{1}$ is the 2×2 unit matrix. We can abbreviate the notation and write

$$H = \begin{bmatrix} h_c & h_{cv} \\ h_{vc} & h_v \end{bmatrix}, \quad (2)$$

with $h_{cv} = h_{vc}$.

Our goal is to obtain effective, single-band Hamiltonians for conduction and valence bands, and the associated effective masses, from the multi-band Dimmock Hamiltonian, eq.

(1). The detail procedure is explained below. Similar reasoning have been used in Ref. 3. The eigenvalue equation from eq. (2) reads

$$\begin{bmatrix} h_c & h_{cv} \\ h_{vc} & h_v \end{bmatrix} \begin{pmatrix} F_c \\ F_v \end{pmatrix} = E \begin{pmatrix} F_c \\ F_v \end{pmatrix}, \tag{3}$$

where Fc and Fv are the envelope function of conduction and valence band, respectively. Equation (3) is equivalent to equation set

$$h_c F_c + h_{cv} F_v = E F_c, \tag{4}$$

$$h_{vc} F_c + h_v F_v = E F_v. \tag{5}$$

From equation (5), we have $(E - h_v)F_v = h_{vc}F_c \rightarrow F_v = (E - h_v)^{-1} h_{vc} F_c$, replacing the last term in equation (4) we obtain an effective Hamiltonian for the conduction band

$$[h_c + h_{cv}(E - h_v)^{-1} h_{vc}] F_c = E F_c. \tag{6}$$

Similarly, for the valence band one obtains

$$[h_v + h_{vc}(E - h_c)^{-1} h_{cv}] F_v = E F_v. \tag{7}$$

If we write $\Delta = (\frac{E_g}{2} + \frac{\hbar^2 k_t^2}{2m_t^+} + \frac{\hbar^2 k_z^2}{2m_l^+})$, then $h_v = -\Delta \mathbb{1}$ and $(E - h_v)^{-1} = \frac{1}{E+\Delta}\mathbb{1}$. Carriers in NPLs are confined within it, then if we consider the case of confinement in the z direction, $(E - h_v)^{-1} = F\mathbb{1}$, and $F = \frac{1}{E+\Delta}$.

With these considerations, and simplifying the notation $\frac{\hbar}{m}P \equiv P$, then we can write

$$
\begin{aligned}
h_{cv}(E-h_v)^{-1}h_{vc} &= [P_l k_z \sigma_z + P_t k_x \sigma_x + P_t k_y \sigma_y]F \\
&\times [P_l k_z \sigma_z + P_t k_x \sigma_x + P_t k_y \sigma_y], \\
&= F[P_l^2 k_z^2 + P_t^2 k_t^2]\mathbb{1} + P_l^2 k_z F k_z \mathbb{1} \\
&+ i\sigma_y (F P_l P_t k_z k_x - F P_l P_t k_x k_z) \\
&+ i\sigma_y P_l P_t k_z F k_x + i\sigma_x (F P_t P_l k_y k_z \\
&- F P_l P_t k_z k_y) - i\sigma_x P_l P_t k_z F k_y \\
&+ i\sigma_z (F P_t^2 k_x k_y - F P_t^2 k_y k_x).
\end{aligned}
\tag{8}
$$

Due to commutativity of the linear momentum components, most terms disappear from the above equation, and we have

$$
\begin{aligned}
h_{cv}(E-h_v)^{-1}h_{vc} &= \mathbb{1}(P_l^2 k_z F k_z + P_t^2 F k_t^2) \\
&- i P_l P_t k_z (F)(\sigma \times k_t \cdot \hat{z}),
\end{aligned}
\tag{9}
$$

where $\hat{z}$ is a unitary vector on z direction. The second term is of Rashba type[4,5] and vanishes except in asymmetric heterojunctions. Thus equation (6) is given by

$$
\left[\frac{E_g}{2} + \frac{\hbar^2 k_t^2}{2m_t^e} + \frac{\hbar^2 k_z^2}{2m_l^e}\right] F_c = E F_c, \tag{10}
$$

where $m_t^e = \left(\frac{1}{m_t^-} + \frac{2P_t^2 F}{m^2}\right)$ and $m_l^e = \left(\frac{1}{m_l^-} + \frac{2P_l^2 F}{m^2}\right)$. Then the effective Hamiltonian, in the single band approximation, looks like a variable mass Hamiltonian with masses having the energy eigenvalues from the 4-band Dimmock Hamiltonian, which allows us to introduce the interaction between conduction and valence bands (similar results are obtained for the valence band from eq. 7). So, considering that the masses are only variable with the position, we have

$$H = -\frac{\hbar^2}{2}\left(\frac{d}{dx}\frac{1}{m_\perp}\frac{d}{dx} + \frac{d}{dy}\frac{1}{m_\perp}\frac{d}{dy} + \frac{d}{dz}\frac{1}{m_z}\frac{d}{dz}\right) + V(x,y,z). \tag{11}$$

The effective masses of a single band can be obtained, but ultimately depend on the energies of the multiband calculation. Knowing that the substitution is possible, for efficiency reasons instead of substituting one by one the terms that relate the single band masses with the terms of the multiband, we will make calculations of a single band and we will find which effective masses fit better to those obtained by the multiband Dimmock calculation.

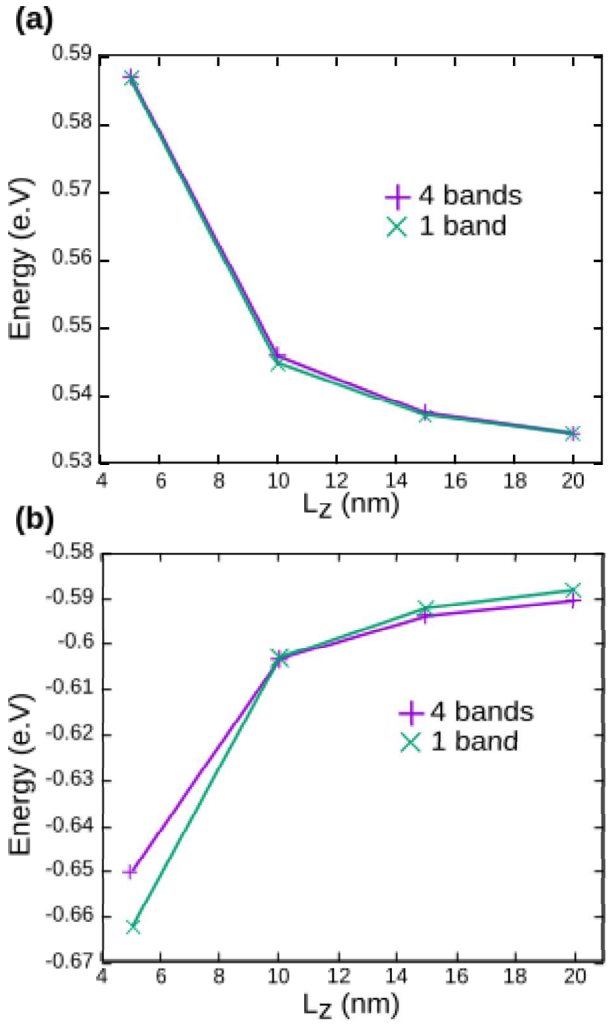

Figure 1: Electron (a) and hole (b) energy as a function of the NPL lateral confinement. The single-band result is the best fit to the full (four-band) calculation, which allows us to propose effective masses. The effective masses found by the single Hamiltonian fit are $m_x^* = 0.29$ ($m_x^* = 0.25$) and $m_{yz}^* = 0.27$ ($m_{yz}^* = 0.19$) for electrons (holes).

In Fig. 1. we fit the effective masses, from the single band Hamiltonian, that have the smallest deviation compared to the calculation of 4-bands Hamiltonian in the L_z range. In this case, the energy was calculated for a NPL with dimensions $L_x = 1.8$ nm, $L_y = 50$ nm. Parameters used in Dimmock Hamiltonian are reported in Ref. 1. The effective masses found by the single Hamiltonian fit are $m_x^* = 0.29$ and $m_{yz}^* = 0.27$ for electrons and $m_x^* = 0.25$ and $m_{yz}^* = 0.19$ for holes. These masses are similar to those obtained for orthorhombic PbS using DFT calculations (Table III in the main text).

Energy Bands with PBE functional

Here we show the energy bands (Fig. 2.) and the effective masses obtained by the PBE functional (TABLE 1), which are similar to those obtained by the PBEsol functional (Fig. 3 main text).

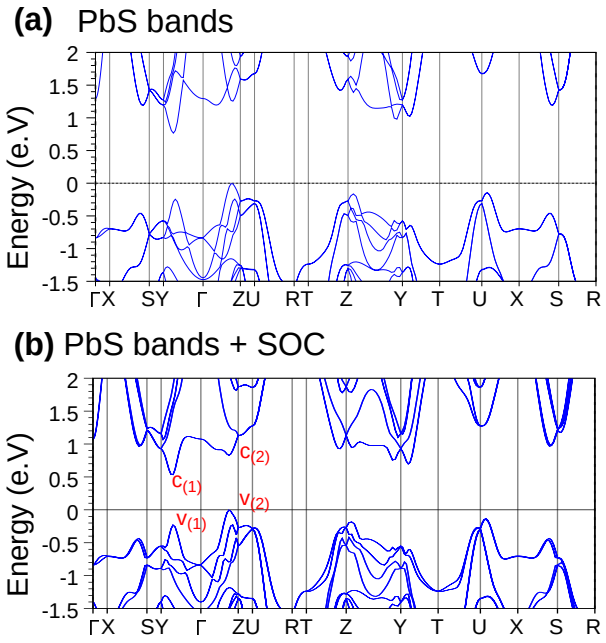

Figure 2: **(a)** Energy bands without and **(b)** with SOC by PBE functional.

Table 1: Effective Masses obtained from energy bands with PBE+SOC. m_0 is the free electron mass.

BAND	**Effective Mass (m_0)**		
	$\mathbf{m_x^*}$	$\mathbf{m_y^*}$	$\mathbf{m_z^*}$
$c_{(1)}$	0.303	0.149	0.159
$c_{(2)}$	0.286	0.251	0.282
$v_{(1)}$	0.405	0.156	0.171
$v_{(2)}$	0.70	0.248	0.206

Rock-Salt PbS Band Structure

We calculate energy bands for the rock-salt structure with the PBEsol functional and the SOC inclusion. We relaxed the structure until forces less than 0.001 R_y/a_0. The first Brillouin zone was sampled with a Γ-centered Monkhorst-pack grid of 6x6x6 k points. A direct gap $E_g = 0.24$ e.V is found at the point of symmetry L, which is clearly underestimated with respect to the reported experimental value (0.42 e.V).

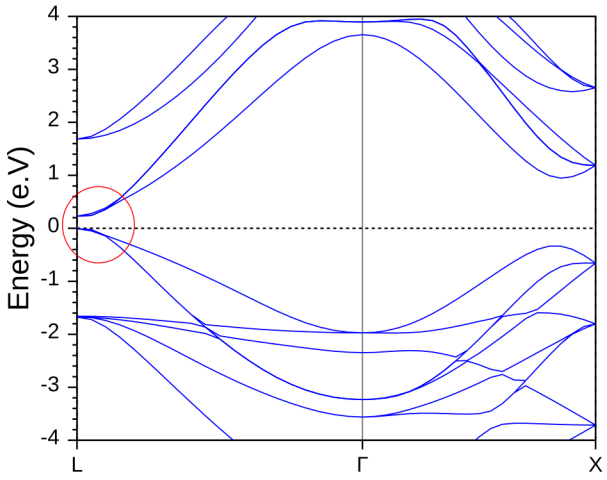

Figure 3: **(a)** Energy bands for PbS rock-salt structure from the PBEsol functional and SOC.

From energy bands we obtained the effective masses $m_x^* = 0.31$ ($m_x^* = 0.25$) and $m_{yz}^* = 0.27$ ($m_{yz}^* = 0.32$) for electrons (holes). These effective masses are similar to those obtained by fitting to a single band (section I) evidencing the validity of the model and reinforcing the value of the effective masses obtained for the orthorhombic case.

Experimental Characterization

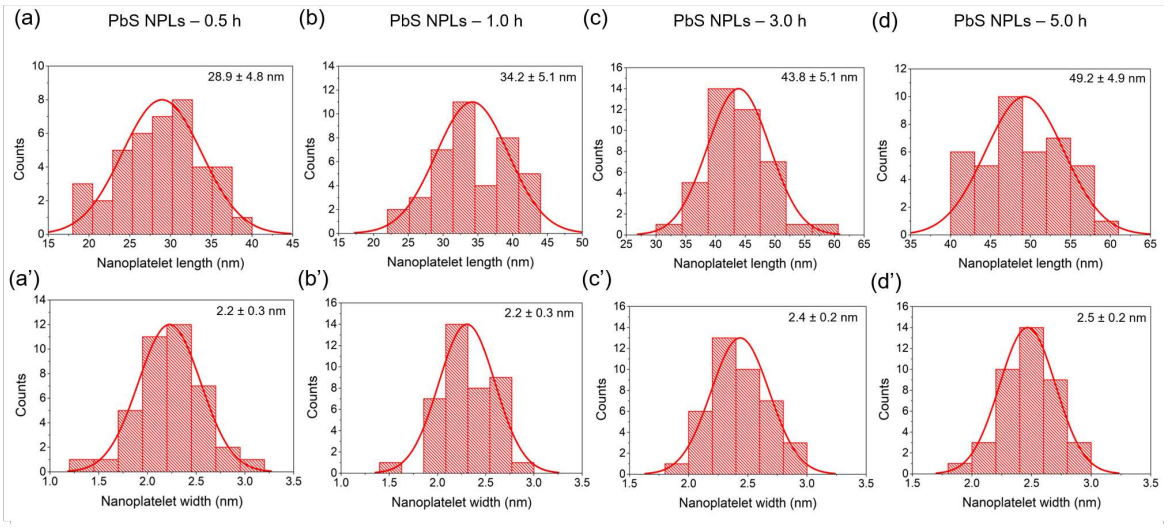

Figure 4: Histograms of the average length and width of PbS NPLs synthesized at different times of reaction: **(a,a')** 0.5 h, **(b,b')** 1.0 h, **(c,c')** 3.0 h and **(d,d')** 5.0 h.

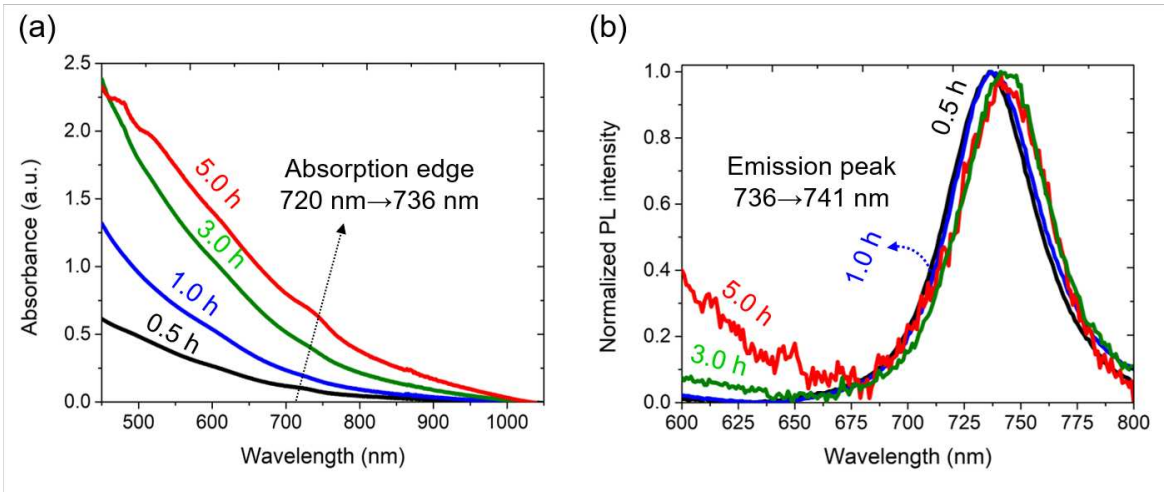

Figure 5: UV-Vis absorption and PL spectra of the PbS NPLs synthesized at different times of reaction: 0.5 h, 1.0 h, 3.0 h and 5.0 h.

Energy Bands of Quasi-tetragonal cell parameters

We calculate the energy bands of bulk PbS from cell parameters $a = 11.9$ Å, $b = 4.22$ Å, $c = 4.2$ Å,[6] with the PBEsol functional and SOC. In Fig. 6 a direct gap is appreciated and the energy bands are in close agreement with those reported in Ref. 6 by the hybrid HSE06 exchange-correlation functional.

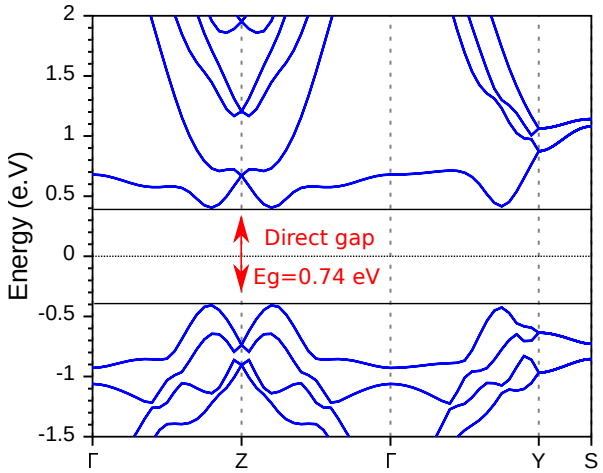

Figure 6: PbS bulk energy bands with quasi-tetragonal cell parameters, PBEsol functional and SOC.

References

(1) Kang, I.; Wise, F. W. Electronic structure and optical properties of PbS and PbSe quantum dots. *JOSA B* **1997**, *14*, 1632–1646.

(2) Masi, S.; Echeverría-Arrondo, C.; Salim, K. M.; Ngo, T. T.; Mendez, P. F.; López-Fraguas, E.; Macias-Pinilla, D. F.; Planelles, J.; Climente, J. I.; Mora-Sero, I. Chemi-Structural Stabilization of Formamidinium Lead Iodide Perovskite by Using Embedded Quantum Dots. *ACS Energy Letters* **2020**, *5*, 418–427.

(3) Yang, J.; Wise, F. Electronic states of lead-salt nanosheets. *The Journal of Physical Chemistry C* **2015**, *119*, 26809–26816.

(4) Winkler, R. Spin-orbit coupling effects in two-dimensional electron and hole systems. *Springer Tracts in Modern Physics* **2003**, *191*, 1–8.

(5) Peter, Y.; Cardona, M. *Fundamentals of semiconductors: physics and materials properties*; Springer Science & Business Media, 2010.

(6) Akkerman, Q. A.; Martín-García, B.; Buha, J.; Almeida, G.; Toso, S.; Marras, S.; Bonaccorso, F.; Petralanda, U.; Infante, I.; Manna, L. Ultrathin Orthorhombic PbS Nanosheets. *Chemistry of Materials* **2019**, *31*, 8145–8153.